UNIVERSITY OF
BATH

University of Bath

Investigation of the H_2O sensing mechanism of DC-operated chemiresistors based on graphene oxide and thermally reduced graphene oxide

Sotirios Papamatthaiou, *Graduate Student Member, IEEE*, Dimitrios-P. Argyropoulos, Filippos Farmakis, and Nikolaos Georgoulas

Abstract— Graphene oxide (GO) is a promising material for H_2O vapour sensing. However, H_2O sensing mechanisms are still under investigation especially in the case of thermally reduced GO. To this purpose, planar devices were fabricated by spin-coating graphene oxide on glass substrates. Ultra high response to H_2O was recorded but poor repeatability and stability over time were also noted. Three different degrees of thermal reduction were applied to improve material stability. An inverse change of resistance was observed for reduced graphene oxide compared to pure graphene oxide upon interaction with H_2O. The sensing mechanisms that govern GO and reduced GO behaviour were studied based on DC measurements. In the case of GO, strong ionic conductivity was proposed whereas in the case of reduced GO mixed electronic/ionic with the leading mechanism affected by H_2O percentage in air, degree of material reduction and sensor working temperature. Finally, it was found that by promoting one sensing mechanism over the other, improved operating humidity range of the sensor can be achieved.

Index Terms— Reduced graphene oxide, relative humidity sensor, thermal reduction, ionic conduction, electronic conduction, activation energy

I. INTRODUCTION

IN the past years, significant advances in semiconductor gas sensors have been announced [1], [2]. The detection of gas molecules is vital for various applications ranging from environmental and chemical warfare protection to medical diagnostics and industrial manufacture [3]-[5]. Relative humidity (RH) measurement is one of the most important issues in the above-mentioned areas of applications [6]. The amount of water vapor that is present in the air can affect not only personal comfort but can also affect various manufacturing processes at industrial applications. For instance, in the semiconductor industry, moisture or humidity levels must be accurately monitored and controlled to ensure proper wafer processing. Humidity control is also important for incubators, respiratory equipment, sterilizers and biological products. In addition, the presence of water vapor may also influence various other chemical, biological and physical processes. More than that, the interest for low consumption, fast response and highly sensitive humidity sensors is ever-growing considering energy demanding applications in harsh environments like portable, wearable devices used outdoors.

Nano-scale materials are considered to be remarkably promising for gas sensing applications thanks to their unique electronic and physical properties. Their high surface to volume ratio potentially offers high sensitivity and low detection limit because the number of the available molecular binding spots is in the order of magnitude of the sensing material molecules. Carbon based nanomaterials, especially graphene and carbon nanotubes have attracted most of the interest and compete for the dominance against other nanomaterials exhibiting advantages like transparency, flexibility and most notably low working temperature [7]-[9]. Graphene oxide (GO), a functionalized form of graphene, has demonstrated a major potential for humidity sensing owing to the abundance of hydrophilic groups. It is generally accepted that GO's poor electrical conductivity is mainly governed by adsorbed-water-induced ions, while it presents poor electronic conductivity [10]-[13]. This explains the resistance decrease upon interaction with humid environment [10], [12]. Nonetheless, mixed electronic/ionic behaviour was reported [14], [15]. However, GO humidity sensors face long-term stability problems and poor repeatability, as it has been suggested in previous works [12], [16]-[18]. Alternatively, reduced or partially reduced graphene oxide (rGO) could be a sufficiently stable material for RH sensing [16], [17], [19]. According to studies [19]-[21], the resistance of rGO, being a p-type semiconductor material, increases when it is exposed to humid environment as water generally acts as electron donor. The reduction of oxygen functional groups leads to decreased ionic conductivity and the simultaneous recovery of sp^2 structure assists the electronic conductivity.

It has to be stressed that the task of this paper is to investigate

S. Papamatthaiou was with the Department of Electrical and Computer Engineering, Democritus University of Thrace, Xanthi, 67100 Greece. He is now with the Centre for Biosensors, Bioelectronics and Biodevices (C3Bio), Department of Electronic and Electrical Engineering, University of Bath, BA2 7AY UK (e-mail: spapamat@gmail.com).

D-P. Argyropoulos, F. Farmakis and N. Georgoulas are with the Department of Electrical and Computer Engineering, Democritus University of Thrace, Xanthi, 67100 Greece (dimiargy56@gmail.com; farmakis@ee.duth.gr; ngeorgou@ee.duth.gr).

the influence of the sensing mechanisms to the behaviour of the DC-operated devices and explore methods enabling the control of this influence. Examination of the H_2O sensing behaviour based on DC-measurements, without the aid of AC complex impedance spectroscopy, was also reported by Popov et al. [22] and Smirnov et al. [23] for devices which exhibited mixed ionic/electronic conduction. Our devices demonstrate low power consumption (e.g. 3.5 $\mu W/cm^2$ against more than 40 mW/cm^2 for commercial ones) making them ideal for battery powered applications, whereas AC mode operation would compromise this advantage and introduce complicated signal processing circuits. Herein, we suggest controllable relation between ionic and electronic conductivity for thermally reduced GO by varying the extent of reduction and the device working temperature. Thus, we propose a technical approach to promote the dominance of a single conduction mechanism for improved sensor performance.

II. MATERIALS AND METHODS

GO films were deposited by spin coating on glass substrates, and aluminum contacts were evaporated on top of the GO through a metal mask in order to form a planar resistive device as Fig.1 (b) shows (ITO was grown in a previous work for a transparent, alternative version [16]). Atomic Force Microscopy revealed film thickness of 85±15 nm. Once the device was prepared, three different thermal reduction steps under forming gas (H_2/N_2: 5/95) were performed at different samples as follows: one sample was lightly annealed up to 180 °C for 10 min (rGO1), another was mildly annealed up to 180 °C for 120 min (rGO2) and finally another one was highly annealed up to 500 °C for 30 min (rGO3). More details on the fabrication and process parameters are presented elsewhere [16]. The experimental setup is illustrated in Fig.1 (a). Electrical measurements were executed in a vacuum test chamber in alternating rough vacuum (3 × 10^{-2} mbar) and laboratory's humid air environment (13-65% RH) at variable temperature (23 °C - 127 °C) using an integrated hot plate. Dry air flow was used to create a controlled low RH environment (<30%) in the vacuum test chamber with the aid of a mass flow controller (Tylan 2900). We have to note that both dry air flow and vacuum were tested to create a dry environment inside the chamber (similar to the experiments reported by Smith et al. [24]) resulting in remarkably similar device behaviour between the two recovery methods. This strongly indicates that it is the humidity that is sensed and there is no pressure influence. However, vacuum was preferred over dry air due to the faster recovery time, as Fig.1 (c) shows. In order to monitor the RH, a commercial humidity sensor (Honeywell's HiH-4000-3) was set up along with our device. For testing the devices at high RH conditions, they were exposed to high RH (>85%) for at least 450 s using a cool mist ultrasonic air humidifier (Capriccio T-253). The electrical behaviour of the fabricated devices under RH exposure and vacuum conditions was tested by applying a constant bias voltage of 7 V and by monitoring the current with a source-meter unit (Keithley

2450). DC-operated humidity sensors have been reported using a bias voltage of higher than 7 V [22], [25]. For our case, a DC voltage of 7 V was necessary for the highly resistive GO. The same bias voltage was applied to rGO for consistency reasons, even though a lower value of 1 V was also tested exhibiting the same sensing behaviour. It has to be noted that linear current-voltage (I-V) curves were extracted exhibiting good ohmic behaviour and no current drift is observed upon voltage application for all cases, indicating no interference from polarization effect. The sensing response of the fabricated devices to RH is defined as $(R-R_0)/R_0$ (%), where R represents the real-time device electrical resistance in the vacuum test chamber and R_0 is the device electrical resistance at a reference RH level (specified for each case). In-house software was used to control the experimental setup and to acquire the data.

III. RESULTS AND DISCUSSION

A. Physical/electrical characterization

X-ray photoelectron spectroscopy (XPS) was conducted to GO and rGO2 devices in our previous work [16] confirming the successful reduction of the material as the C-C bonds represent 50% and 90% of the total C- bonds for GO and rGO2 respectively. The removal of oxygen groups restores the π-network and the conductivity is recovered. Sheet resistances of GO and rGO were extracted under vacuum (23 °C) by sweeping the DC-voltage and recording the current. In all cases, ohmic behaviour was observed. GO is the most resistive of the four devices with 1.86 × 10^7 MΩ/sqr. RGO1 follows with 89.65 MΩ/sqr whereas rGO2 and rGO3 are less resistive with 10.88 MΩ/sqr and 4.72 MΩ/sqr, respectively. Since the sample sheet resistance values inversely scale with the thermal reduction temperature and duration, it can be considered that the extracted sheet resistance is a straightforward indication of the reduction level of the rGO layer.

B. RH sensing with GO

It has been shown that upon interaction with humidity GO resistance decreases [10], [12], [26]. This behaviour was also observed in our GO devices for both medium and high RH level. Fig.2 shows the evolution of GO resistance when exposed to low-to-mid and high RH level. The sensing response of GO from vacuum (resistance of 7 × 10^5 MΩ) to 35% RH (resistance of 6 × 10^3 MΩ) is more than 10^4 % whereas the response from vacuum to 95% RH (resistance of 52 MΩ) is more than 10^6 %, rendering it the most sensitive resistive GO humidity sensing device using DC measurement in the literature: 4.6 × 10^4 % for a RH change of 84% in [10] and 35.5% in [17] for a RH change of 95%. It has to be highlighted that the GO sensor signal fully recovers after high RH exposure and no permanent water absorption was detected that would require possible heating cycles to revert.
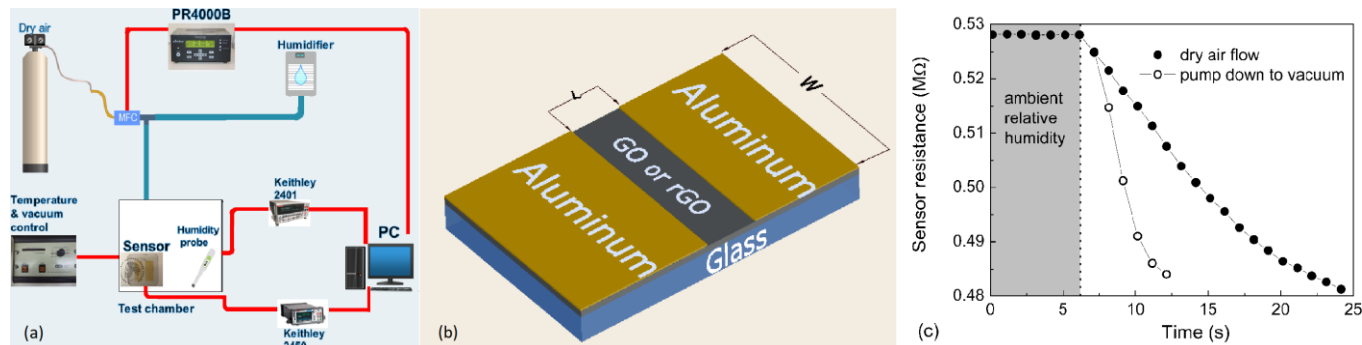
Fig. 1. (a) Schematic layout of the experimental setup, (b) sensor schematic (L = 0.9 mm, W = 24 mm) and (c) resistance versus time for rGO2 sensor during dry air flow and pumping down to vacuum. Similar behaviour was observed in all tested devices.

It is known that the decrease of the GO resistance upon exposure to RH is due to ionic or protonic conduction induced by the interaction of H_2O molecules with the GO flakes [10], [12]. GO acts as an electronic insulator due to its disrupted sp^2 bonds. However, the oxygen functional groups (i.e. carboxylic, hydroxyl, epoxide) which are present in GO behave as hydrophilic sites that play a substantial role to ionic conductivity. It can be considered that as soon as GO comes in contact with humid air, H_2O molecules are chemically adsorbed (chemisorption) at the oxide surface forming a layer of hydroxyls [6], [27]. Consequently, the additional water molecules that will approach form the first physisorbed layer on the available sites. These physisorbed water molecules are relatively hard to move due to the double hydrogen bonding created between the water molecule and the hydroxyls and ionic conductivity is minimal [6], [26]-[29]. With further increase of adsorbed water molecules at the material, single bonding of water to hydroxyls takes place and forms the second and succeeding physisorbed layers of water while hydrogen bonds are also formed between water molecules. These water molecules become mobile and thus the less-ordered structure starts to resemble more a liquid-like rather than an ice-like of the first layer. From this point and as RH reaches high levels, apart from the proton and hydroxide (OH) hopping transfer (Grotthuss proton and hydroxide transfer mechanism) [30] , hydronium (H_3O^+) charge transfer becomes dominant due to the substantial amount of accumulated water molecules ($H_2O+H_2O \Leftrightarrow H_3O+OH^-$), which in return will dissociate into H_2O passing the proton to an adjacent H_2O molecule ($H_3O^++H_2O \Leftrightarrow H_2O+H_3O^+$). This significantly decreases sensor's electrical resistance [27]. More than that, the interlayer penetration of water molecules in the GO will further facilitate the hydrolysis of more functional groups and the generation of water channels among the GO layers (taking advantage of the increased interlayer distance of the GO [31]). Thus, this mechanism leads to the aforementioned extreme sensing response at high RH [26].

Even though the GO device exhibits huge response to RH, it lacks long-term stability and repeatability. GO seems to diminish its ability to sense water vapours over a short period of time (less than a week) after fabrication. Moreover, an inconsistent sensing behaviour regarding the magnitude of the response at back-to-back sensing cycles can be observed in

Fig.2 (a). These two drawbacks are crucial for a gas sensor and the deficiency of them makes any sensor unreliable and, thus, undesirable for use. Similar behaviour of material instability was also observed at previous works [12], [17], [18], [32]. A reasonable explanation for the compromised sensing response over time, which is also supported by the
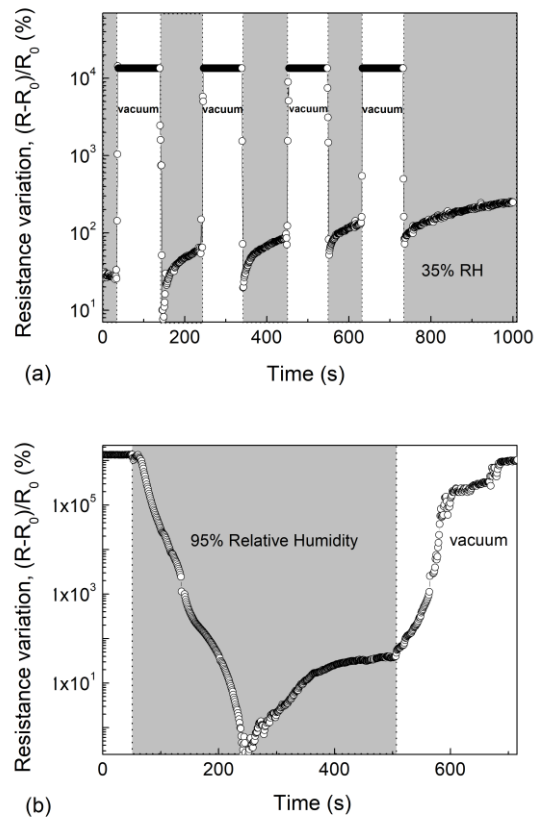

Fig. 2. Resistance variation for GO sensor at 23 °C (a) in alternating vacuum-air environment (35% RH) and (b) before, during and after high relative humidity exposure.

fading response at successive sensing cycles, is the destructive role that the adsorption and desorption of water molecules play to the structural properties of the GO sheets. It has been found that the stacking of the GO sheets provokes a hostile environment for the creation of water channels as the interlayer distance decreases [33]. It could be assumed that the adsorption and desorption of water molecules may influence

mechanically the GO weakening its structure. Indeed, continuous cycling of water molecules through GO may escalate the material stacking leading to minimised interlayer distance for water adsorption and decreased response to RH. In order to improve the stability of the sensor, thermal reduction was applied.

C. RH sensing with rGO

The resistance evolution of the three rGO devices when exposed to selected RH levels in alternating air-vacuum environment is shown in Fig.3. The resistance is decreased for all reduced devices as soon as vacuum is created, in contrast to the GO's aforementioned behaviour. It is clear that the resistance recovers its previous value when RH is returned to humid air after vacuum on all three devices indicating sustaining sensing behaviour regarding stability and repeatability. This behaviour applies to all tested levels of RH up to 65%. Moreover, the sensing responses of rGO1 and rGO2 are not increased upon raising the H_2O concentration in air. For rGO1, a sensing response of 23% is noticed at 32% RH whereas a sensing response of 5.5% is observed at 55% RH. Similarly, rGO2 decreases its response from 17.5% to 16% at 48% RH and 56% RH, accordingly. However, the sensing response of the highly reduced sensor (rGO3) does not follow this behaviour, as it increases from 5.3% at 32% RH to 7.5% at 57% RH. The calibration curves of the three rGO devices are shown in Fig.4. It is seen that the response scales inversely with the reduction level of the rGO up to 40-45 % of RH. However, this does not apply for higher RH exposures. Indeed, the calibration curve for lightly reduced rGO1 sample reveals a declining response pattern for increasing RH levels over 40%, which is not observed for the other two samples (rGO2 and rGO3). For mildly reduced rGO2, a declining response pattern can be observed for RH levels greater than 48%, displaying also a more gradual downward inclination than rGO1. Interestingly, highly reduced rGO3 does not seem to exhibit similar behaviour, instead a wider sensing range is achieved.

From the above observations, it can be suggested that the dominant sensing mechanism of rGO to water vapours is the electron transfer induced by the interaction of the analyte and the sensing material. From previous works [19]-[21], it has been proven that thermally reduced GO act as a p-type semi-conductive material. In our case, by using the hot-probe method [34], it was found that all devices, independently of the reduction method, exhibited p-type semiconductor behaviour. Since water is a poor oxidizing and reducing agent, it behaves accordingly to the surrounding environment. Water generally serves as electron donor upon its interaction with rGO [19], [20]. Hence, the donated electrons from water decrease rGO hole-dominated current. In addition, it is also clear that this interaction is correlated to the oxygen groups of graphene oxide. Indeed, it was seen that devices with lower content of oxygen groups exhibit lower sensing response. Thus, we believe that the oxygen groups act like trapping sites for the water molecules.
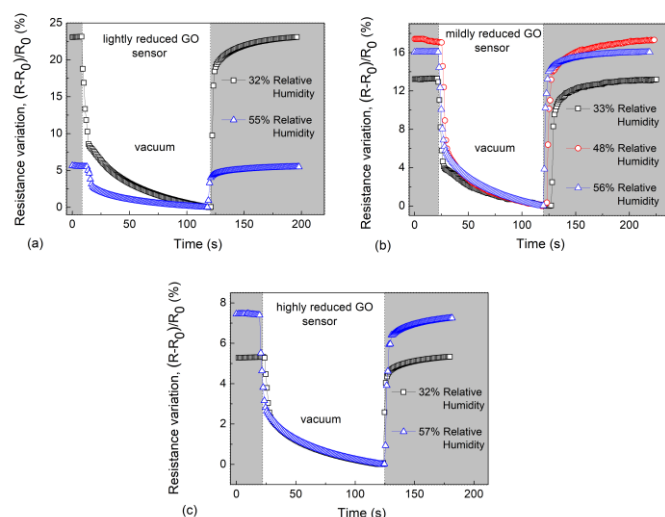

Fig. 3. Resistance variation in alternating air-vacuum environment at 23 °C for rGO (a) lightly reduced (180 °C for 10 min, rGO1), (b) mildly reduced (180 °C for 120 min, rGO2) and (c) highly reduced (500 °C for 30 min, rGO3).
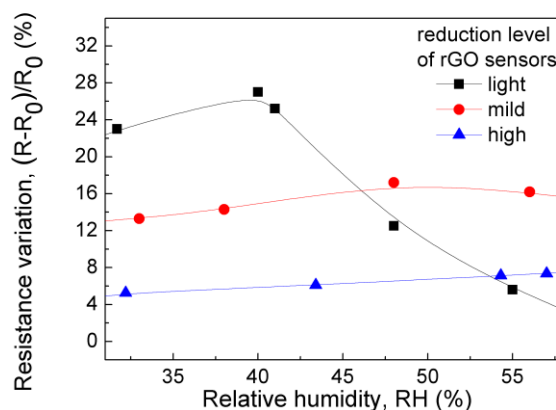

Fig. 4. Resistance variation for rGO (square: lightly reduced (rGO1), circle: mildly reduced (rGO2), triangle: highly reduced (rGO3)) sensors monitored versus relative humidity at 23 °C. R_o is the resistance at vacuum.

In order to further investigate the rGO behaviour regarding the steep and the moderate direction change of the calibration curve for rGO1 and rGO2 respectively, all reduced devices were exposed to high RH levels. Fig.5 (a)-(c) shows the response of the three rGO devices before (ambient 32% RH and vacuum), during (>85% RH) and after (ambient 32% RH) high RH exposure. It has to be noted that the reference condition represents ambient RH. Originally, material's resistance is stable as the RH is maintained at 32%. As soon as vacuum is created the resistance is decreased for all reduced devices, as expected from the previously described behaviour in Fig.3. Lightly reduced rGO1 exhibits 22% sensing response between vacuum and 32% RH environment, whereas the more heavily reduced devices exhibit lower response, i.e. 13% for mildly reduced rGO2 and 5% for highly reduced rGO3.
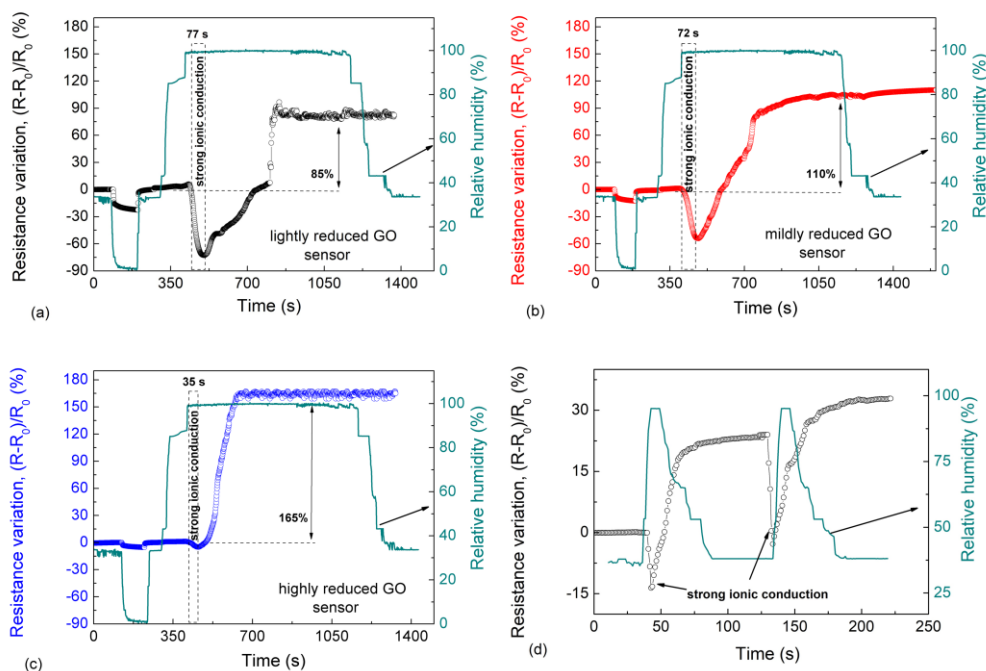
Fig. 5. Evolution of resistance at 23 °C for rGO sensor (a) lightly reduced (180 °C for 10 min, rGO1), (b) mildly reduced (180 °C for 120 min, rGO2) and (c) highly reduced (500 °C for 30 min, rGO3) before (ambient and no humid environment), during and after high relative humidity exposure; (d) evolution of resistance for rGO2 as a function of time in alternating ambient-human exhale (10 cm distance from the device) environment. Left axis represents rGO resistance variation and right axis the relative humidity level in the test chamber. R_o is the resistance at ambient conditions (before the high relative humidity exposure).

However, when sensors are exposed to higher than 85% of RH, a complex behaviour is observed, similar for all tested devices. Initially, sensor resistance is sharply decreased, demonstrating opposite behaviour than the one observed during medium RH exposure. Then, after certain duration, it starts to increase and abruptly reaches a maximum value which remains unchanged even when the devices are brought back to environmental RH values.

More particularly, during the first phase upon high RH exposure, the resistance is decreased at most by 73% for rGO1, 54% for rGO2 and 5% for rGO3 after 77 s for rGO1, 72 s for rGO2 and 35 s for rGO3. We have to note that the above values seem to scale with reduction level of the rGO. During the second phase, while sensors remain exposed to high RH, the resistance on all three devices is increased by 85% (rGO1), 110% (rGO2) and 165% (rGO3) compared to their initial values. This behaviour to high RH is attributed to absorbed water molecules which could possibly affect carrier mobility (water swelling effect [35]) and/or carrier concentration.

An identical behaviour to high RH was observed when the devices were exposed to human exhale (saturated with water) 10 cm from the device lasting 3 s and 4 s for the first and second attempt respectively. Fig.5 (d) shows the abrupt resistance decrease of rGO2 (14% for a 3 s exhale and 27% for a 4 s exhale) when the exhale is performed followed by a permanent increase (24% after the first exhale for 3 s and 8% further increase after the second exhale for 4 s).

From the above results, it can be deduced that the oxygen groups play a significant role to the dominant sensing mechanism (electronic versus ionic conductivity) especially

when the devices are subjected to high RH conditions. This becomes evident when the RH is increased over 85% and the resistance of all tested devices is abruptly decreased in agreement to GO's behaviour shown in Fig.2, designating high ionic conductivity induced by the physisorbed water molecules. The resistance change for the most reduced device (rGO3) is lower compared to the less reduced one (rGO1) and this can be attributed to the corresponding oxygen groups that facilitate ionic conductivity. This is further supported by the fact that the rGO samples exhibit similar behaviour to the GO samples only when they are exposed to high RH. Therefore, it can be assumed that the ionic conductivity is enhanced by the presence of oxygen groups through hopping mechanism. It has to be noted that the abrupt resistance decrease upon high RH exposure may originate not only by the increase of ionic conductivity but also by simultaneous decrease of electronic conductivity due to the insulating effect of water layers to the electron transport between adjacent sheets [36].

Finally, when the samples are brought back to ambient RH conditions (32%), the dissimilarity of the permanent resistance increase between the three devices due to the swelling effect may be caused by the increased material defects. Defects are created when carbon backbone is consumed by releasing CO and CO_2 at high reducing temperatures [37]. These defects are expected to be more numerous in the highly reduced sample (rGO3) and could be significant in allowing the interlayer trapping of water molecules that leads to permanent swelling effect.

Regarding the behaviour under human exhale, Fig.5 (d) highlights the suitability of rGO for applications that require

sensing of short bursts of water saturated air since the resistance is decreased abruptly and the effect of swelling is not capable to hamper the response in such a short duration of exposure.

Considering these findings, the declining response pattern for rGO2 but mainly for rGO1 after a certain RH level in Fig.4 could be explained by the competition between electronic and ionic conductivity which is affected by the reduction level (and thus the oxygen group content) of the GO. As previously discussed, ionic conductivity is enhanced by the oxygen functional groups and RH level of the environment. After a certain RH level, ionic conduction is considerable enough to create an inverse response (resistance decrease) compared with the response due to electron donation (resistance increase). Therefore, in the case of rGO1, the ionic conduction mechanism is enhanced, steering the balance between ionic and electronic conduction towards the former at the low-to-mid RH range. It is remarkable that rGO1 response is lower than rGO3 at 55% RH due to the competition of these two conduction mechanisms. For further reduced samples (rGO2 and rGO3) where the oxygen groups are diminished, the sensing response to RH decreases as the material becomes less favourable for H_2O trapping but the competition between the two conduction mechanisms becomes less pronounced, as rGO2's calibration curve exhibits a decrease for higher %RH level than rGO1, whereas no such behaviour is seen for rGO3's. The opposite response to low-medium RH between GO and rGO sensors and the maximum range of operating range for each sensor are highlighted in Table 1.

TABLE I
THE MAXIMUM VALUE OF OPERATING RANGE FOR EACH DEVICE AND THE DEPENDENCE OF SENSOR RESPONSE SIGN ON THE DEGREE OF MATERIAL THERMAL REDUCTION AND RELATIVE HUMIDITY.

Device	GO	rGO1	rGO2	rGO3
Degree of reduction	No (as deposited)	Lightly reduced	Mildly reduced	Highly reduced
ΔR $(R-R_{vac})$ sign at low-medium RH	< 0	> 0	> 0	> 0
ΔR $(R-R_{vac})$ sign at high RH	< 0	< 0	< 0	< 0
Maximum value of operating range	99% RH	40% RH	48% RH	65% RH

In order to further study the kinetics of both conduction mechanisms and their dependence on the temperature, we performed electrical measurements at a temperature range between 27 °C and 127 °C under humid and non-humid environment as displayed in Fig.6. The devices were heated up to 127 °C and their electrical resistance was monitored by cooling down to room temperature at 10 °C interval steps. It has to be noted that the devices were maintained at every temperature step for a sufficient time in order to obtain a stabilized resistance value. It is clear that two temperature ranges can be distinguished: one where the response sign from humid air (35% RH) to vacuum is positive and one where this sign turns to negative. In both regimes edges, the response value corresponds to the degree of the material reduction: highest for rGO1 (35% @ 27 °C and -53.3% @ 127 °C),

lowest for rGO3 (8.3% @ 27 °C and -6% @ 127 °C) and rGO2 in the middle (16% @ 27 °C and -41.8% @ 127 °C). It is also interesting to note the temperature at which the response sign changes from positive to negative. For both rGO1 and rGO2, the sign changes after the two lower temperature steps, between 37 °C and 47 °C. However, in rGO3 case the sign changes after the fifth step, between 67 °C and 77 °C.
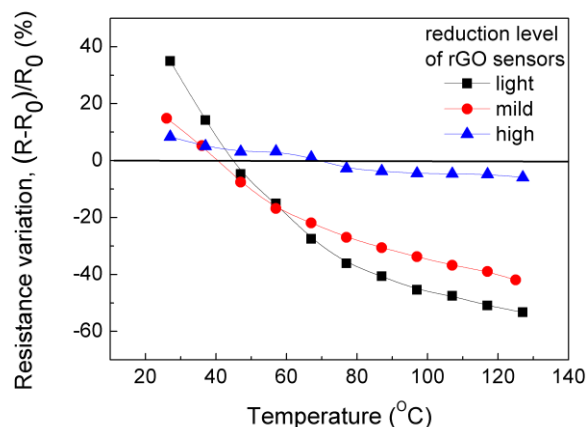

Fig. 6. Resistance variation for rGO sensor (square: lightly reduced (rGO1), circle: mildly reduced (rGO2), triangle: highly reduced (rGO3)) in alternating air (35% RH)-vacuum environment, monitored versus temperature.

Based on the above observations, positive response sign at the low temperature region is explained by the previously described electron donation from water to rGO. Yet, it is noted that the sign of the response at elevated temperatures changes to negative. This is similar to the change of the response sign at high RH that is discussed in Fig.5 and the compromise of the response after a certain level of RH for rGO1 and rGO2 in Fig.4. Thus, it is attributed to the enhancement of the ionic conductivity from the increase of temperature, which is consistent with the results reported by others [14], [38], [39] resulting from the enhanced motion of ions and water molecules. This influence of temperature to the ionic conductivity and consequently to the dominant conduction mechanism is affected by the degree of reduction and therefore by the amount of oxygen functional groups in the material which are responsible for the interaction with H_2O molecules. Similarly, the shift of the temperature point at which ionic conduction dominates over electronic (response sign becomes negative) is affected by the degree of reduction as, in a more reduced material, ionic conduction requires more temperature boost to dominate. This working temperature dependency could be beneficial from the sensor perspective because depending on the temperature region that the sensor works, electronic (low temperature region) or ionic conduction (high temperature region) will be promoted and the competition between them will be alleviated expanding the RH sensing range.

Finally, for further investigation of ionic conductivity at this temperature range, ln(R) was plotted against 1/T for vacuum and humid air (35% RH) and Arrhenius equation was used to calculate E_A from the slope of the linear fitting function. As

Fig.7 shows, it was found that E_A decreases with reduction at the same environment conditions as 0.0823 eV for rGO1 is decreased to 0.0276 eV for rGO3 and 0.1927 eV for rGO1 is decreased to 0.0423 eV for rGO3 at vacuum and humid air, respectively. In addition, E_A is increased at humid air compared to vacuum for all reductions.
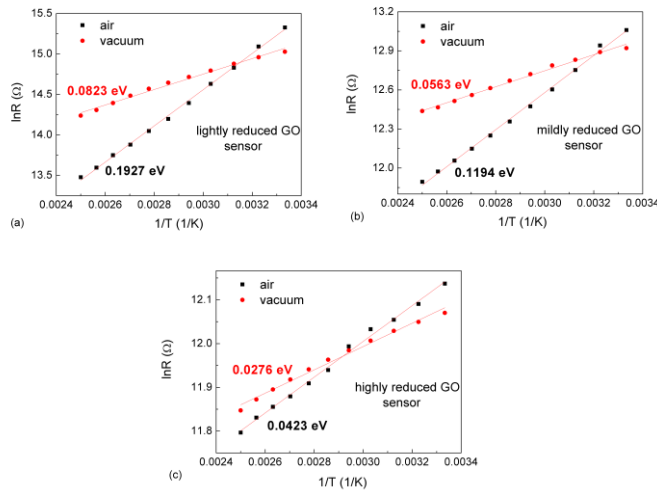

Fig. 7. Arrhenius curves with the activation energies for lightly (rGO1), mildly (rGO2) and highly reduced (rGO3) devices at vacuum and humid (35% RH) environment.

It can be assumed that E_A at vacuum is mostly related to the electronic conduction as practically no interaction with air molecules is possible [14]. Reduction alters the material to a more electronically conductive material and for this reason the E_A at vacuum is decreased with reduction. The fact that E_A at humid air is greater than E_A at vacuum indicates that there is a contribution of ionic conductivity to this sum, taking into account that E_A for ionic conductivity is expected to be higher than E_A for electronic [14]. More than that, E_A at humid air for rGO1 and rGO2 agrees well with reported values for ionic conductivity ruled by Grotthuss mechanism [14], [39]. Additionally, the percentage of E_A attributed to electronic conductivity, to the total E_A at humid air, increases with the degree of reduction from 42.7% for rGO1 to 47.2% for rGO2 and 65.2% for rGO3 designating the inverse relationship of ionic conductivity with reduction.

IV. CONCLUSION

In summary, three different degrees of thermal reduction were applied to GO devices in order to improve the repeatability and stability over time. Mixed electronic and ionic conductivity in rGO is proposed to explain the increase and decrease of resistance upon exposure to different RH % levels. Temperature dependency of the dominant conduction mechanism was presented and activation energies in the range of 127 °C to 27 °C were calculated for humid and non-humid environment acting as a further proof of mixed electronic/ionic conductivity. The degree of reduction and the working temperature of the sensitive devices define the dominant conduction mechanism at a certain RH % level.

Finally, even though rGO's sensitivity is compromised, it can be considered as an alternative material for ambient RH sensing applications on account of the low power consumption and transparency.

REFERENCES

[1] *Expanding the vision of sensor materials*. Washington, D.C.: National Academy Press, 1995.
[2] S. E. Zohora, A. M. Khan, and N. Hundewale, "Chemical Sensors Employed in Electronic Noses: A Review," *Advances in Computing and Information Technology Advances in Intelligent Systems and Computing*, pp. 177–184, 2013.
[3] D. Kohl, "Function and applications of gas sensors", *J. Phys. D: Appl. Phys.*, vol. 34, no. 19, pp. R125-R149, Sept. 2001.
[4] S. Ryabtsev, A. Shaposhnick, A. Lukin and E. Domashevskaya, "Application of semiconductor gas sensors for medical diagnostics", *Sens. Actuators B, Chem.*, vol. 59, no. 1, pp. 26-29, Oct. 1999.
[5] A. Ponzoni, C. Baratto, S. Bianchi, E. Comini, M. Ferroni, M. Pardo, M. Vezzoli, A. Vomiero, G. Faglia and G. Sberveglieri, "Metal Oxide Nanowire and Thin-Film-Based Gas Sensors for Chemical Warfare Simulants Detection", *IEEE Sens. J.*, vol. 8, no. 6, pp. 735-742, Jun. 2008.
[6] H. Farahani, R. Wagiran and M. Hamidon, "Humidity Sensors Principle, Mechanism, and Fabrication Technologies: A Comprehensive Review", *Sensors*, vol. 14, no. 5, pp. 7881-7939, Apr. 2014.
[7] K. Xu, C. Fu, Z. Gao, F. Wei, Y. Ying, C. Xu, and G. Fu, "Nanomaterial-based gas sensors: A review," *Instrumentation Science & Technology*, vol. 46, no. 2, pp. 115–145, Jul. 2017.
[8] R. Bogue, "Nanomaterials for gas sensing: a review of recent research", *Sensor Review*, vol. 34, no. 1, pp. 1-8, 2014.
[9] E. Llobet, "Gas sensors using carbon nanomaterials: A review", *Sens. Actuators B, Chem.*, vol. 179, pp. 32-45, Mar. 2013.
[10] Y. Yao, X. Chen, J. Zhu, B. Zeng, Z. Wu and X. Li, "The effect of ambient humidity on the electrical properties of graphene oxide films", *Nanoscale Res. Lett.*, vol. 7, no. 1, p. 363, Jul. 2012.
[11] S. Borini, R. White, D. Wei, M. Astley, S. Haque, E. Spigone, N. Harris, J. Kivioja and T. Ryhänen, "Ultrafast Graphene Oxide Humidity Sensors", *ACS Nano*, vol. 7, no. 12, pp. 11166-11173, Nov. 2013.
[12] G. Naik and S. Krishnaswamy, "Room-Temperature Humidity Sensing Using Graphene Oxide Thin Films", *Graphene*, vol. 05, no. 01, pp. 1-13, Jan. 2016.
[13] J. Nie, Y. Wu, Q. Huang, N. Joshi, N. Li, X. Meng, S. Zheng, M. Zhang, B. Mi, and L Lin, "Dew Point Measurement Using a Carbon-Based Capacitive Sensor with Active Temperature Control", *ACS Appl. Mater. Interfaces*, vol. 11, no. 1, pp. 1699-1705, Jan. 2019.
[14] T. Bayer, S. Bishop, N. Perry, K. Sasaki and S. Lyth, "Tunable Mixed Ionic/Electronic Conductivity and Permittivity of Graphene Oxide Paper for Electrochemical Energy Conversion", *ACS Appl. Mater. Interfaces*, vol. 8, no. 18, pp. 11466-11475, Apr. 2016.
[15] K. Hatakeyama, M. Islam, K. Michio, C. Ogata, T. Taniguchi, A. Funatsu, T. Kida, S. Hayami and Y. Matsumoto, "Super proton/electron mixed conduction in graphene oxide hybrids by intercalating sulfate ions", *J. Mater. Chem. A*, vol. 3, no. 42, pp. 20892-20895, Sept. 2015.
[16] S. Papamatthaiou, D. Argyropoulos, F. Farmakis, A. Masurkar, K. Alexandrou, I. Kymissis and N. Georgoulas, "The Effect of Thermal Reduction and Film Thickness on fast Response Transparent Graphene Oxide Humidity Sensors", *Procedia Engineering*, vol. 168, pp. 301-304, Dec. 2016.
[17] D. Phan and G. Chung, "Effects of rapid thermal annealing on humidity sensor based on graphene oxide thin films", *Sens. Actuators B, Chem.*, vol. 220, pp. 1050-1055, Dec. 2015.
[18] A. Dimiev, L. Alemany and J. Tour, "Graphene Oxide. Origin of Acidity, Its Instability in Water, and a New Dynamic Structural Model", *ACS Nano*, vol. 7, no. 1, pp. 576-588, Dec. 2012.
[19] D. Zhang, J. Tong and B. Xia, "Humidity-sensing properties of chemically reduced graphene oxide/polymer nanocomposite film

sensor based on layer-by-layer nano self-assembly", *Sens. Actuators B, Chem.*, vol. 197, pp. 66-72, Jul. 2014.

[20] C. Chen, X. Wang, M. Li, Y. Fan and R. Sun, "Humidity sensor based on reduced graphene oxide/lignosulfonate composite thin-film", *Sens. Actuators B, Chem.*, vol. 255, pp. 1569-1576, Feb. 2018.

[21] G. Lu, L. Ocola and J. Chen, "Gas detection using low-temperature reduced graphene oxide sheets", *Appl Phys Lett.*, vol. 94, no. 8, p. 083111, Feb. 2009.

[22] V. Popov, D. Nikolaev, V. Timofeev, S. Smagulova and I. Antonova, "Graphene-based humidity sensors: the origin of alternating resistance change", *Nanotechnology*, vol. 28, no. 35, p. 355501, Jul. 2017.

[23] V. Smirnov, A. Mokrushin, V. Vasiliev, N. Denisov and K. Denisova, "Mixed proton and electron conduction in graphene oxide films: field effect in a transistor based on graphene oxide", *Appl. Phys. A*, vol. 122, no. 5, May 2016.

[24] A. Smith, K. Elgammal, F. Niklaus, A. Delin, A. Fischer, S. Vaziri, F. Forsberg, M. Råsander, H. Hugosson, L. Bergqvist, S. Schröder, S. Kataria, M. Östling and M. Lemme, "Resistive graphene humidity sensors with rapid and direct electrical readout", *Nanoscale*, vol. 7, no. 45, pp. 19099-19109, Oct. 2015.

[25] L. Wang, Y. He, J. Hu, Q. Qi and T. Zhang, "DC humidity sensing properties of BaTiO3 nanofiber sensors with different electrode materials", *Sens. Actuators B, Chem.*, vol. 153, no. 2, pp. 460-464, Apr. 2011.

[26] H. Bi, K. Yin, X. Xie, J. Ji, S. Wan, L. Sun, M. Terrones and M. Dresselhaus, "Ultrahigh humidity sensitivity of graphene oxide", *Scientific Reports*, vol. 3, no. 1, Sept. 2013.

[27] Y. Yeh, T. Tseng and D. Chang, "Electrical Properties of Porous Titania Ceramic Humidity Sensors", *J. Am. Ceram. Soc.*, vol. 72, no. 8, pp. 1472-1475, Aug. 1989.

[28] S. Misra and N. Pandey, "Study of activation energy and humidity sensing application of nanostructured Cu-doped ZnO thin films", *J. Mater. Res.*, vol. 31, no. 20, pp. 3214-3222, Sept. 2016.

[29] N. Yamazoe and Y. Shimizu, "Humidity sensors: Principles and applications", *Sens. Actuators*, vol. 10, no. 3-4, pp. 379-398, Nov. 1986.

[30] N. Agmon, "The Grotthuss mechanism", *Chem. Phys. Lett.*, vol. 244, no. 5-6, pp. 456-462, Oct. 1995.

[31] K. Hatakeyama, S. Hayami and Y. Matsumoto, "Graphene Oxide Based Electrochemical System for Energy Generation", in *Inorganic Nanosheets and Nanosheet-Based Materials*, T. Nakato, J. Kawamata and S. Takagi, Ed. Tokyo: Springer, 2017, pp. 331-346.

[32] J. Paredes, S. Villar-Rodil, A. Martínez-Alonso and J. Tascón, "Graphene Oxide Dispersions in Organic Solvents", *Langmuir*, vol. 24, no. 19, pp. 10560-10564, Aug. 2008.

[33] X. Li, X. Chen, X. Chen, X. Ding and X. Zhao, "High-sensitive humidity sensor based on graphene oxide with evenly dispersed multiwalled carbon nanotubes", *Mater Chem Phys*, vol. 207, pp. 135-140, Mar. 2018.

[34] A. Axelevitch and G. Golan, "Hot-probe method for evaluation of majority charged carriers concentration in semiconductor thin films", *Facta universitatis - series: Electronics and Energetics*, vol. 26, no. 3, pp. 187-195, Dec. 2013.

[35] S. Papamatthaiou, D. Argyropoulos, A. Masurkar, M. Cavallari, F. Farmakis, I. Kymissis and N. Georgoulas, "Permanent water swelling effect in low temperature thermally reduced graphene oxide", *Appl Phys Lett.*, vol. 110, no. 25, p. 252106, Jun. 2017.

[36] D. Wang, A. Du, E. Taran, G. Lu and I. Gentle, "A water-dielectric capacitor using hydrated graphene oxide film", *J Mater Chem*, vol. 22, no. 39, p. 21085, Sept. 2012.

[37] R. Larciprete, S. Fabris, T. Sun, P. Lacovig, A. Baraldi and S. Lizzit, "Dual Path Mechanism in the Thermal Reduction of Graphene Oxide", *J. Am. Chem. Soc.*, vol. 133, no. 43, pp. 17315-17321, Aug. 2011.

[38] B. Zhang, Y. Cao, S. Jiang, Z. Li, G. He and H. Wu, "Enhanced proton conductivity of Nafion nanohybrid membrane incorporated with phosphonic acid functionalized graphene oxide at elevated temperature and low humidity", *J Membrane Sci*, vol. 518, pp. 243-253, Nov. 2016.

[39] M. Karim, K. Hatakeyama, T. Matsui, H. Takehira, T. Taniguchi, M. Koinuma, Y. Matsumoto, T. Akutagawa, T. Nakamura, S. Noro, T. Yamada, H. Kitagawa and S. Hayami, "Graphene Oxide Nanosheet with High Proton Conductivity", *J. Am. Chem. Soc.*, vol. 135, no. 22, pp. 8097-8100, May 2013.

S. Papamatthaiou (M'18) was born in Komotini, Greece, in 1992. He received his B.Eng and M.Sc. degrees in Electrical and Computer Engineering from Democritus University of Thrace, Xanthi, Greece in 2015 and 2017, respectively. Currently, he is pursuing the PhD degree in the Department of Electronic and Electrical Engineering, University of Bath, UK. His research interests include gas sensors, bio-sensors, lab on chip and surface functionalization.

D-P. Argyropoulos was born in Xanthi, Greece, in 1990. He received his B.Eng and M.Sc. degrees in Electrical and Computer Engineering from Democritus University of Thrace, Xanthi, Greece in 2015 and 2017, respectively, where he is currently pursuing the PhD degree. His research interests include material characterization, micro-fabrication and lithium-ion batteries.

F. Farmakis received his B.S. degree in Physics from Aristotle University of Thessaloniki, Greece, in 1996, the M.Sc. degree from National Polytechnic School of Grenoble, France, in 1997 and his Ph.D. from the same School in 2000. Currently, he is Assistant Professor at the Democritus University of Thrace (D.U.TH.), Electrical and Computer Engineering Department in Xanthi, where he pursues research on gas sensor technology and lithium-ion batteries. He is the author and co-author of more than 50 scientific papers in refereed international journals and conferences.

N. Georgoulas received the diploma degree in Electrical and Computer Engineering (Dipl.-Ing.) from the department of Electrical and Computer Engineering, Technical University of Munich (TUM), Germany, in 1978 and the Ph.D. Degree (Dr.-Ing) from the same department in 1981. Since 2008 he is the Director of the Laboratory of Electrical and Electronic Materials Technology in the Electrical and Computer Engineering Department, D.U.TH. Professor Georgoulas served as the Head of Electrical and Computer Engineering Department for two consecutive terms (1997-1999 and 1999-2001), as member of the Deanship (1997-2001), as member of the Senate (1997-2001) and as member of the Research Committee of D.U.TH. (1997-2003). He was also a member of the strategic planning Committee of D.U.TH., and he has established the Carrier and Business Office of the institution (1997). His scientific interests are mainly focused in Microelectronic and Nanoelectronic technology. In these areas he has published more than 55 papers in international scientific peer reviewed journals and conferences and has participated in more than 18 research and development projects.